Compensating Power Amplifier Distortions on Radar Signals via Waveform Design

Ehsan Raei, Mohammad Alaee-Kerahroodi, Bhavani Shankar M. R., Björn Ottersten

Interdisciplinary Centre for Security, Reliability and Trust (SnT), University of Luxembourg, Luxembourg

Email: {ehsan.raei, mohammad.alaee, bhavani.shankar, bjorn.ottersten}@uni.lu

Abstract—This paper aims to study the distortion effect of Power Amplifiers (PAs) on radar waveforms in terms of Integrated Sidelobe Level in Single Input and Single Output (SISO) radar systems. To this end, we consider Memory Polynomial (MP) model as behavior of the PA which considers both non-linearity and memory distortions. Then, we consider minimizing the auto-correlation of the PA output in the baseband as a design metric for compensating the distortion effect of the PA. In this regard, we proposed an algorithm based on Coordinate Descent (CD) method to design an M-ary Phase Shift Keying (MPSK) waveform, which is a discrete phase waveform. Finally, in the numerical results, we evaluate the performance of the proposed method and compare it with Digital Predistortion (DPD) method as a conventional approach for compensating the distortion effect of PA.

Index Terms—Waveform Design, Power Amplifier (PA), Memory Polynomials, Optimization, Coordinate Descent (CD), M-ary Phase Shift Keying (MPSK)

I. INTRODUCTION

Waveforms play an important role in the behavior and performance of radar and communication systems, and their design has gotten a lot of attention in order to improve the performance of radar and communication systems [1]. In radar systems, a waveform with a low auto-correlation sidelobes is used to avoid masking weak targets in the range sidelobes of a strong return [2], and also to mitigate the harmful effects of distributed clutter returns near the target of interest [3]. Low auto-correlation sidelobes are desired in communication systems for synchronization and to reduce multi-access interference [1]. On the other hand low cross-correlation level is desired to obtain orthogonality in Code-Division Multiple Access (CDMA) Multiple-Input Multiple-Output (MIMO) radar systems [4]–[6]. In general, the most common metrics for designing a waveform with good sidelobes level are Integrated Sidelobe Level (ISL) and Peak Sidelobe Level (PSL) [2]. In this regard, several constant modulus waveforms are known which have low ISL/PSL, including, Barker, Linear Frequency Modulation (LFM), Frank, and Golomb sequences.

Recently, radar technology has advanced significantly in antenna design, Radio Frequency (RF) transceivers, and signal processing techniques, as part of an ongoing revolution with significant momentum. However, the destructive effects of Power Amplifier (PA)s on transmit waveforms are unavoidable

and serve as a source of error generation for a variety of systems.

Conceptually, a PA is an active electronic device that provides an amplified and undistorted version of its low-power RF input waveform at its output. In other words PAs should act as a wideband and linear system. However, the PAs contain non-idealities that can cause performance degradation of the systems they drive when deployed in the real world [7], [8]. Such distortions can significantly impair the system's expected performance, particularly in radar applications involving spectrum-sharing strategies to enable coexistence between radar and other telecommunication systems operating in the same frequency band. Indeed, out-of-band spurious components have the potential to degrade the performance of systems operating in frequency bands adjacent to the radar's. Furthermore, if the designed radar waveform includes notches in the frequency spectrum, in-band distortion could seriously compromise the depth of the nulls, resulting in spectral compatibility issues with overlaid systems. [9], [10]. This non-ideality behavior is more intensive when we try to obtain higher output power from PAs, especially near the saturation region.

In order to compensate this non-idialities, we need to model the PA behavior properly. In general, the non-ideality behavior of PAs is modelled into memory-less (non-linearity) and considering memory effect, respectively.

A. Memory-less distortion models

These models assume that the PA is only dependent on the instant input, i.e. the PA output is independent of the previous input samples. These models usually express the non-ideality output of a PA as a non-linear function of its input. Fig. 1 shows the non-linearity behavior of a PA. Based on this figure, the PA curve is linear when the input power is between a Sensitivity level and IP1 dB value. Beyond that, by increasing the input level, the output level will be entered into the non-linear region and converges to a saturation power. This effect is usually described by the amplitude and phase transfer characteristic of the PA. The first and the latter are often referred to Amplitude Modulation/Amplitude Modulation (AM/AM) and Amplitude Modulation/Phase Modulation (AM/PM) conversion of the PA respectively. There are several models to describe the non-linearity behavior of PAs including, cubic polynomial, Saleh, Ghorbani and Rapp models, just to list a few [11]–[13].
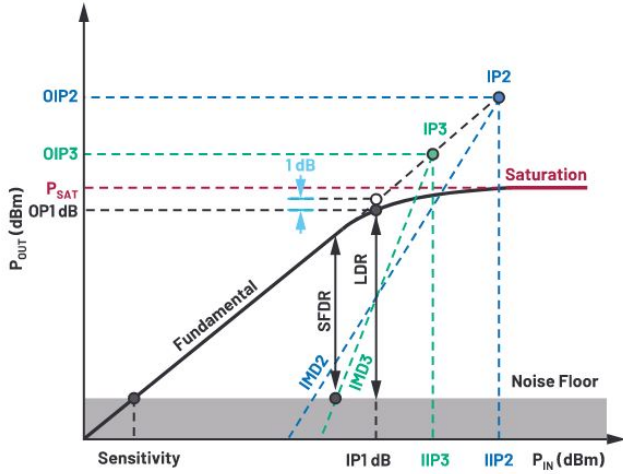
Fig. 1: The non-linearity behavior of PA [14].

B. Non-linearity with memory distortion models

These models not only consider the instant effect of the input signal but also consider the effect of previous samples in the output of PAs. There are some models to describe the non-linearity with memory in PA, such as Volterra and Memory Polynomial (MP) models [9], [10].

C. Digital Predistortion

To mitigate this degradation, linearization algorithms including Digital Pre-Distortion (DPD) can be applied as part of the transmitter or receiver chain. DPD is a cost-effective linearization technique that aims to provide improved linearity, better efficiency, and take full advantage of PAs. In general, DPD applies inverse distortion, at the input signal of the PA to cancel the distortion generated by the PA. DPD algorithms aim to preemptively distort the waveform to be transmitted to counter the nonlinear effects of the PA. This requires knowledge about the PA characteristics accurately with effective implementation for successful DPD functioning.

D. Contribution

Best of our knowledge, no study has been done to evaluate the impact of PA distortion on sidelobes of radar waveform. In this paper, via waveform design, we consider compensating the distortion effect of PA in Single-Input Single-Output (SISO) radar systems. In this regard, we consider the MP model to estimate the behavior of PA and then design an M-ary Phase Shift Keying (MPSK) waveform to obtain a low ISL for the PA output. To optimize the waveform, we propose an algorithm based Coordinate Descent (CD) under discrete phase constraint. The optimization of the waveform also leads to a significant reduction in the out-of-band emission. This results in efficient spectrum utilization and enhances radar and communication operations.

E. Paper Organization

The rest of this paper is organized as follows. In Section II, we introduce the system model and formulate an optimization problem to design a waveform for compensating the harmful effect of PA distortion. The CD framework is developed in Section III to solve the problem efficiently. Section IV provides numerical experiments to evaluate the performance of the proposed method.

F. Notations

This paper uses lower-case and upper-case boldface for vectors ($\mathbf{a}$) and matrices ($\mathbf{A}$) respectively. The set of complex numbers, transpose, conjugate transpose, Frobenius norm, and absolute value are denoted by $\mathbb{C}$, $(.)^T$, $(.)^H$, $\|.\|_F$ and $|.|$ symbols respectively. The letter j represents the imaginary unit (i.e., $j = \sqrt{-1}$), while the letter (i) is used as a step of a procedure. Finally, $\circledast$ denotes cross-correlation operator.

II. SYSTEM MODEL AND PROBLEM FORMULATION

Let $\mathbf{x} \in \mathbb{C}^N$ be a base-band transmitted waveform in SISO radar system with length of N as follow:

$$\mathbf{x} = [x_1, x_2, \ldots, x_N]^T \in \mathbb{C}^N \qquad (1)$$

Let us assume that $\mathbf{y} \in \mathbb{C}^N$ be the PA output when we feed it with the waveform $\mathbf{x}$. In this case considering the MP model with non-linearity order of K and memory depth of M, the nth sample of PA output can be written as the following equation [10]:

$$y(n) = \sum_{q=0}^{Q-1} \sum_{m=0}^{M-1} a_{q,m} x_{(n-m)} |x_{(n-m)}|^q. \qquad (2)$$

In (2), $a_{q,m}$ are the coefficient of MP model and depend on temperature, input power and frequency of PA.

In order to compensate for the distortion effect of PA, DPD is one of the cost-effective linearization techniques. It features a linearization capability to preserve overall efficiency, and it takes full advantage of advances in digital signal processors and A/D converters. The technique adds an expanding non-linearity in the baseband that complements the compressing characteristic of the RF PA. Ideally, the cascade of the pre-distorter and the power amplifier becomes linear and a constant gain amplifies the original input. With the pre-distorter, the PAs can be utilized up to its saturation point while maintaining good linearity. In general, the DPD can be seen as an "inverse" of the PA. The DPD algorithm needs to model the PA behavior accurately and efficiently for successful DPD deployment [7], [8].

However, in this paper, we are interested in compensating the PA distortion by deploying a waveform design technique. We consider minimizing the auto-correlation sidelobes of PA output, i.e. $\mathbf{y} = [y_1, \ldots, y_N]^T \in \mathbb{C}^N$. The aperiodic auto-correlation of $\mathbf{y}$ is defined as:

$$r(l) \triangleq \sum_{n=1}^{N-l} y_n y^*_{(n+l)}, \qquad (3)$$

where $l \in \{-N+1, \ldots, N-1\}$ is the lag of cross-correlation. The zero-lag of auto-correlation represents the peak of the

matched filter output and contains the energy of the sequence i.e. $r(0) = \mathbf{y}^H\mathbf{y}$, while the other lags $(l \neq 0)$ are referred to the sidelobes. Thus, the range-ISL of waveform $\mathbf{y}$ can be expressed by [15]:

$$\text{ISL} = f(\mathbf{x}) \triangleq \sum_{l=-N+1}^{N-1} |r(l)|^2 - |r(0)|^2 = \|\mathbf{y} \circledast \mathbf{y}\|_2^2 - \mathbf{y}^H\mathbf{y} \tag{4}$$

Please note that the MP coefficients are unknown and they need to be estimated. To this end, in the first step a known input signal is given to the PA as input then the output is measured. Then with the known input and the measured output, the coefficients can be estimated by Least Square (LS) criterion [7], [8]. Let $\bar{a}_{q,m}$ be the estimated MP coefficients of PA. We are interested in designing a waveform with good ISL of PA output ($\mathbf{y}$). In this regard, we consider solving the following optimization problem:

$$\begin{cases} \min_{\mathbf{X}} & \|\mathbf{y} \circledast \mathbf{y}\|_2^2 - \mathbf{y}^H\mathbf{y} \\ s.t. & y_n = \sum_{q=0}^{Q-1}\sum_{m=0}^{M-1} \bar{a}_{q,m} x_{(n-m)}|x_{(n-m)}|^k \\ s.t. & x_n \in \mathcal{X}_K, \quad \forall n \in \{1,\ldots,N\} \end{cases} \tag{5}$$

where $\mathcal{X}_K$ indicates the discrete phase (MPSK) sequence with K alphabet size. More precisely:

$$\mathcal{X}_K = \{e^{j\phi}|\phi \in \Omega_K\}; \quad \Omega_L \triangleq \left\{0, \frac{2\pi}{K}, \ldots, \frac{2\pi(K-1)}{K}\right\}. \tag{6}$$

Problem (5) is a multi-variable, non-convex and NP-hard optimization problem. In the following, we proposed a CD-based method to obtain a local optimum solution.

III. PROPOSED METHOD

To tackle Problem (5), instead of designing the entire vector $\mathbf{x}$, we consider designing its entries consecutively. CD framework enables such an optimization by assuming one entry of the code vector $\mathbf{x} \in \mathbb{C}^N$ as the variable and keeping the others fixed. Subsequently, by examining all possible alphabet of MPSK for the chosen variable, we obtain all the critical points of the objective function with respect to that variable, and then we update that by selecting the alphabet which leads to the best ISL [2]. We repeat this procedure to update the other entries until we meet the convergence criterion. There are several rules to choose the coordinates to update at each iteration (see [16] for more details). In the following, we enumerate some updating rules:

- **Randomized**: Randomly select some coordinate to update (sample with replacement), i.e., uniformly randomly choose n at each iteration;
- **Cyclic**: Run all coordinates in cyclic order, $n = 1 \rightarrow 2 \ldots \rightarrow N \rightarrow 1 \rightarrow \ldots$, i.e., iterate over these N different x_n;
- **Greedy** (called also Maximum Block Improvement (MBI) or Gauss-Southwell) [17]: Evaluate the objective

value by making update to each x_n separately and choose the best one;
- **Parallel** (Jacobi style): Parallelly update every n at each iteration.

It is worth noting that the greedy selection rule could be costly with a large number of blocks but has faster convergence than randomized/cyclic selection of the variables [18]. Also, we should be careful when using the parallel update rule. In particular, it could happen that updating either x_n or x_m $(m = 1,\ldots,N)$ will decrease the objective, however, updating both x_n; x_m will cause an increase in the objective.

In this paper, we consider using the cyclic rule for updating the variables. To illustrate CD framework let us assume that x_d is the dth transmitted pulse $(d = 1,\ldots,N)$ and is the only variable at i^{th} iteration, while the other $N-1$ entries are fixed; these are stacked into the $\mathbf{x}_{(-d)}^{(i)}$ vector as,

$$\mathbf{x}_{(-d)}^{(i)} = [x_1^{(i)}, \ldots, x_{(d-1)}^{(i)}, x_{(d+1)}^{(i-1)}, \ldots, x_N^{(i)-1}]^T \in \mathbb{C}^{N-1}. \tag{7}$$

where the superscripts (i) and $(i-1)$ show the updated and non-updated entries at i^{th} iteration. The design Problem (5) with respect to the variable x_d can be expressed as,

$$\begin{cases} \min_{x_d} & f\left(x_d, \mathbf{x}_{(-d)}^{(i)}\right) \\ \text{s.t.} & x_d \in \mathcal{X}_L \end{cases}, \tag{8}$$

which is still a non-convex constrained optimization problem; however, unlike the earlier formulation, it involves only one variable. Towards solving this, we calculate ISL for each possible alphabet of x_d and choose the one that results in the best minimum ISL. In the next step, we perform this procedure for the next pulse $(x_{(d+1)})$ and the process is repeated till all pulses are optimized at least once. This optimization procedure is shown in (9) for vector $\mathbf{x}$:

$$x_d^{(i)} = \arg\min_{x_d} f\left(x_d, \mathbf{x}_{(-d)}^{(i)}\right), \quad \forall d \in \{1,\ldots,N\} \tag{9}$$

where $x_d^{(i)}$ denotes the optimum value of x_d at the ith iteration of the optimization procedure. Therefore the optimized vector $\mathbf{x}$ with respect to d^{th} entry at i^{th} iteration can be obtained by:

$$\mathbf{x}_{(d)}^{(i)} = [x_1^{(i)}, \ldots, x_{(d-1)}^{(i)}, x_d^{(i)}, x_{(d+1)}^{(i-1)}, \ldots, x_N^{(i-1)}]^T \in \mathbb{C}^N. \tag{10}$$

Based on the aforementioned discussion, we propose CD framework waveform design to derive the optimum x_d under discrete phase constraint. The summary of the proposed method is given by Algorithm 1. As can be seen, the algorithm is initialized with waveform $\mathbf{x}^{(0)}$ and matrix $\bar{\mathbf{A}}$ where $\bar{\mathbf{A}} \in \mathbb{C}^{M \times Q}$ is the estimated MP coefficients matrix of PA, where its entries consist of $\bar{a}_{q,m}$. Then the algorithm chooses the dth entry and calculates the objective value for each alphabet and saves it in vector $\mathbf{v}$. Since (5) is a discrete optimization problem $\mathbf{v}$ contains the critical points of the problem with respect to x_d. Thus, the optimum solution can be obtained by lines 9) and 10) of the algorithm. **Algorithm 1** optimizes the vector $\mathbf{x}$ entry by entry until all N pulses become optimized at least once. After optimizing the Nth pulse, the algorithm

Algorithm 1 : Waveform design for compensating PA distortion.

Input: $\mathbf{x}^{(0)} \in \mathbb{C}^N$ and $\bar{\mathbf{A}} \in \mathbb{C}^{Q \times M}$.

Initialization: $i := 0$.

Optimization:
1) $i = i + 1$;
2) $\mathbf{x}^{(i)} = \mathbf{x}^{(i-1)}$;
3) **for** $d = 1, \dots, N$ **do**
4) $\mathbf{v} = \mathbf{0}_K$;
5)   **for** $k = 1, \dots, K$ **do**
6) $x_d^{(i)} = e^{j\frac{2\pi(k-1)}{K}}$;
7) $v_k = f\left(\mathbf{x}_{(d)}^{(i)}\right)$; using (4)
8)   **end for**
9) $k^\star = \arg\min_k\{\mathbf{v}\}$;
10) $x_d^{(i)} = e^{j\frac{2\pi(k^\star-1)}{K}}$;
11) **end for**
12) **if** $\left\|\mathbf{x}^{(\mathbf{i})} - \mathbf{x}^{(\mathbf{i-1})}\right\| < \zeta$
13)   Stop;
14) **else**
15)   go to step 1);

Output: $\mathbf{x}^\star = \mathbf{x}^{(i)}$.

(a) Convergence of the Objective Function

(b) Convergence of the arguments

Fig. 2: Convergence of the (a) objective function and (b) argument, with different alphabet size ($N = 256$, $M = 4$ and $Q = 7$)

examines the convergence metric. The algorithm repeats the aforementioned steps if the stopping criterion is not met. We consider $\left\|\mathbf{x}^{(i)} - \mathbf{x}^{(i-1)}\right\| < \zeta$ for stopping criterion of optimization, where ζ is a positive threshold, $\mathbf{x}^{(i)}$ and $\mathbf{x}^{(i-1)}$ are the waveforms in $(i)^{th}$ and $(i-1)^{th}$ iteration, i.e.:
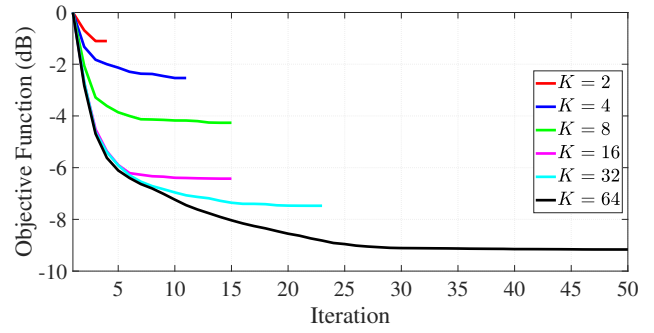
$$\mathbf{x}^{(i)} = [x_1^{(i)}, \dots, x_N^{(i)}]^T \in \mathbb{C}^N$$
$$\mathbf{x}^{(i-1)} = [x_1^{(i-1)}, \dots, x_N^{(i-1)}]^T \in \mathbb{C}^N. \tag{11}$$

Due to the iterative improvement of CD method, this framework guarantees that the ISL converges monotonically to the local optimum value.
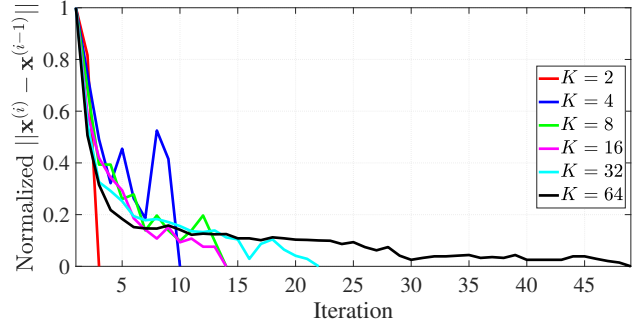
IV. NUMERICAL RESULTS

In this section, we consider evaluating the performance of the proposed method in different aspects. In the first step, we evaluate the convergence behavior of the proposed method. Then we compare its performance with the DPD method as a conventional method for compensating for the distortion behavior of PA. To this end, we use the DPD of communication toolbox in MATLAB to estimate the MP coefficients and perform the DPD pre-distortion to the input signal of PA [19], [20]. Besides, we consider the memory depth and non-linearity order to be $M = 4$ and $Q = 7$ respectively.

As to the **Algorithm 1** parameters, we consider Discrete Phase Modulation (DPM) as the initial sequence [2]. This sequence basically is a phase coded (MPSK) sequence ($\mathbf{x}_0 \in \mathbb{C}^N$) with a good ISL level [2]. DPM it self is initialized with a random phase coded which every code entry is given by, $e^{j\phi_n^{(0)}}$, where $\phi_n^{(0)}$ is a random real and discrete variable uniformly distributed in set $\{0, \frac{2\pi}{K}, \dots, \frac{2\pi(K-1)}{K}\}$. Besides, we

assume that the stopping condition for **Algorithm 1** is set at $\zeta = 10^{-3}$ with maximum iteration of 10^3.

A. Convergence

Fig. 2 shows the convergence behavior of the proposed method in different aspects. In this regard, Fig. 2a shows the convergence of the objective function with different alphabet sizes (K). As can be seen, for all alphabet sizes (K) the objective function decreases monotonically and converges to the optimum value. In addition, the larger alphabet size obtains better performance (lower objective function). Since a larger alphabet size is equivalent to a larger feasible set, this behavior was expected. Fig. 2b shows the convergence of the stopping criterion which basically is the convergence of the argument of the proposed method. Observe that for all alphabet sizes these curves converge to zero. As a result, Fig. 2 and Fig. 2b indicate that the solution converges to a stationary point.

B. Comparing with DPD

This subsection compares the performance of the proposed method and DPD in terms of ISL. Here, we assume that a DPM sequence is the input signal of PA (and the initial waveform of the proposed method) and we termed it as $\mathbf{x}^{(0)}$. Based on DPD technique first, we pre-distorted the input signal ($\mathbf{x}^{(0)}$) and apply it to the PA. Then we compute the cross-correlation of the PA output and $\mathbf{x}^{(0)}$. However, in the proposed method we minimize the ISL of PA output ($\mathbf{y}$) and
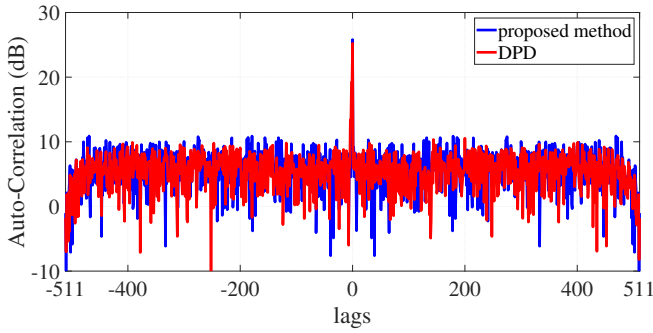
(a) Auto-Correlation
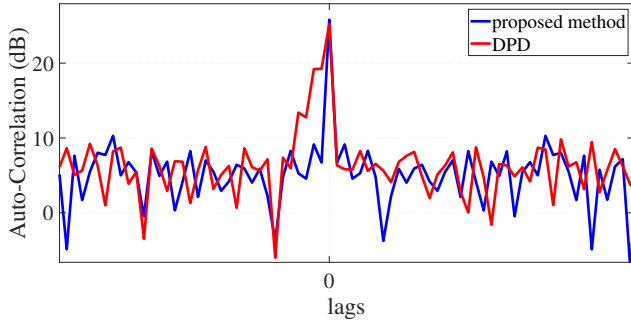
(b) Zoom of Auto-Correlation

Fig. 3: Comparing the Auto-Correlation function of the proposed method and DPD ($N = 512$, $M = 4$ and $Q = 7$)

(a) Averaged of ISL vs sequence length (N)

(b) Averaged of PSL vs sequence length (N)

Fig. 4: Comparing the average of (a) ISL and (b) PSL with 10 number of trials with different sequence length ($M = 4$ and $Q = 7$)

we report its auto-correlation. Please note that unlike $\mathbf{x}^{(0)}$, $\mathbf{y}$ is not a constant modulus waveform, therefore for a fair comparison, we normalized the power of $\mathbf{y}$ to the power of $\mathbf{x}^{(0)}$.

Fig. 3 shows the auto-correlation function of the proposed method and DPD. As can be seen in Fig. 3a, the sidelobes far away from zero lag ($l = 0$), for both methods have similar sidelobe levels. However, Fig. 3b shows the auto-correlation function near the zero lag. As can be seen, the DPD method has larger sidelobes compared to the proposed method. Besides, the proposed method has a higher gain compared to DPD method, i.e. the proposed method offers higher peak in zero lag.
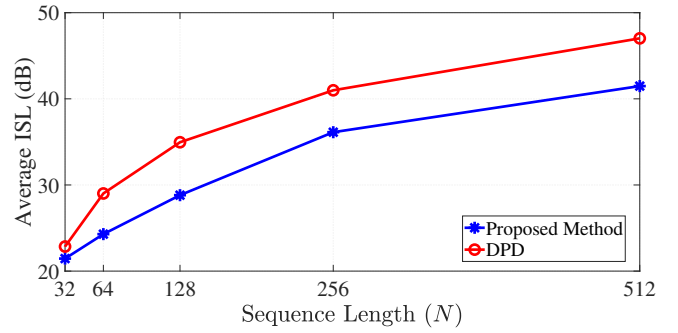
Fig. 4 shows the averaged of ISL and the PSL of the proposed method and DPD with different sequence length (with 10 trials). As can be seen, the proposed method offers lower ISL and PSL in all cases.

Fig. 5 compares the range-Doppler profile of the proposed method with DPD. In this figure we consider nine targets with range and velocity of $t_i = (r_i, v_i), i \in \{1, \ldots, 9\}$. Let us assume that r and v be the sets of range and velocity of the targets respectively. In this regard, we assume the following set up:
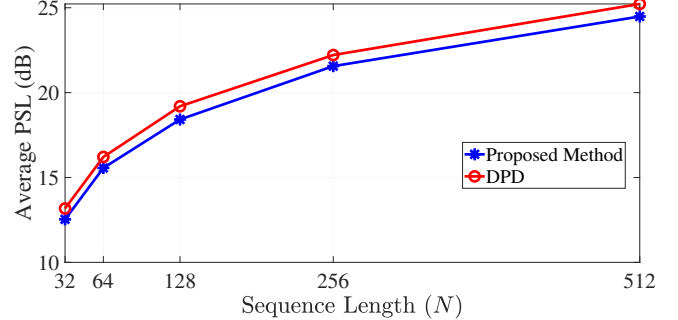
$$r = \{10, 12, 14, 10, 12, 14, 10, 12, 14\} \text{(km)}$$
$$v = \{-10, -10, -10, 0, 0, 0, 10, 10, 10\} \text{(m/sec)}.$$

Fig. 5 shows the range-Doppler profile of DPD and the proposed method. As can be seen, the proposed method (see

Fig. 5a) offers lower sidelobes in both range and Doppler domain compared to DPD method (see Fig. 5b).

Spectrum sharing (shaping) is one of the common approaches for deploying coexistence between radar and other RF transmitters (for example communication system). In this regard, out of band mitigation is crucial in coexistence of radar and communication system scenarios. Fig. 6 compares the out of band spectrum of proposed method and DPD. As can be seen, the proposed method offers lower out of band sidelobes compared to DPD. In addition, the proposed method has a flatter spectrum and is closer to the desired spectrum. This shows that the proposed method uses the available band-width more effectively compared to the DPD.

V. CONCLUSION

This paper investigated the effects of PA on ISL in SISO radar systems. To that end, we consider the MP model to be the behavior of the PA, which takes into account both non-linearity and memory distortions. Then, as a design metric for compensating the PA's distortion effect, we consider minimizing the auto-correlation of the PA output in the baseband. In this regard, we proposed a method based on CD for designing a MPSK (discrete phase) waveform. Finally, in the numerical results, we evaluate the proposed method's performance and compare it to the DPD method, which is a conventional approach for compensating the distortion effect of PA. We show that the proposed method offers lower ISL and PSL than
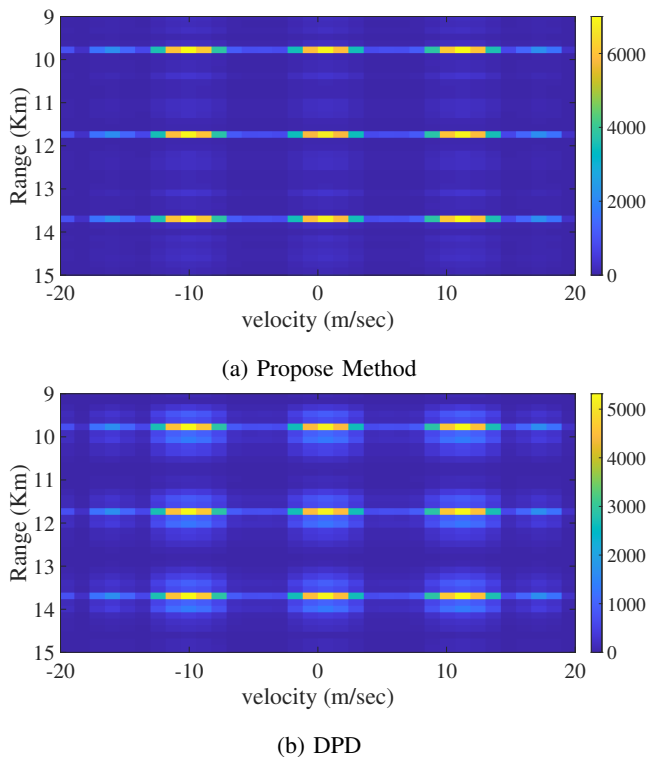
(a) Propose Method

(b) DPD

Fig. 5: Comparing the range-Doppler profile of (a) proposed method and (b) DPD with nine targets ($N = 256$, $M = 4$ and $Q = 7$)
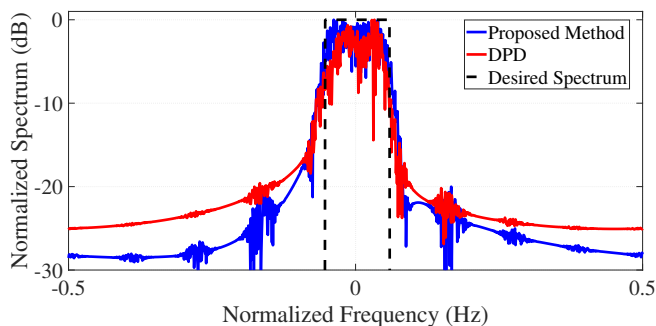

Fig. 6: Comparing the out of band mitigation performance of the proposed method with DPD ($N = 128$, $M = 4$ and $Q = 7$).

DPD. In addition the proposed method has better performance in terms of out of band spectrum mitigation.

REFERENCES

[1] H. He, J. Li, and P. Stoica, *Waveform Design for Active Sensing Systems*. Cambridge University Press, 2012.

[2] M. A. Kerahroodi, A. Aubry, A. De Maio, M. M. Naghsh, and M. Modarres-Hashemi, "A coordinate-descent framework to design low psl/isl sequences," *IEEE Transactions on Signal Processing*, vol. 65, no. 22, pp. 5942–5956, 2017.

[3] C. J. Nunn and G. E. Coxson, "Best-known autocorrelation peak sidelobe levels for binary codes of length 71 to 105," *IEEE Transactions on Aerospace and Electronic Systems*, vol. 44, no. 1, pp. 392–395, 2008.

[4] E. Raei, M. Alaee-Kerahroodi, and B. S. Mysore R, "Spatial- and range-ISLR trade-off in MIMO radar via waveform correlation optimization," *IEEE Trans. Signal Process.*, pp. 1–1, 2021.

[5] E. Raei, S. Sedighi, M. Alaee-Kerahroodi, and M. B. Shankar, "MIMO radar transmit beampattern shaping for spectrally dense environments," *IEEE Trans. Aerosp. Electron. Syst*, pp. 1–13, 2022.

[6] E. Raei, M. Alaee-Kerahroodi, P. Babu, and M. R. B. Shankar, "Design of MIMO radar waveforms based on lp-norm criteria," 2021.

[7] A. Aubry, V. Carotenuto, A. De Maio, A. Farina, A. Izzo, and R. S. L. Moriello, "Assessing power amplifier impairments and digital predistortion on radar waveforms for spectral coexistence," *IEEE Transactions on Aerospace and Electronic Systems*, vol. 58, no. 1, pp. 635–650, 2022.

[8] V. Carotenuto, A. Aubry, A. De Maio, A. Izzo, A. Farina, and R. S. Lo Moriello, "Power amplifier distortions on radar signals for spectral coexistence," in *2021 Signal Processing Symposium (SPSympo)*, 2021, pp. 35–39.

[9] A. Zhu, J. C. Pedro, and T. J. Brazil, "Dynamic deviation reduction-based volterra behavioral modeling of rf power amplifiers," *IEEE Transactions on Microwave Theory and Techniques*, vol. 54, no. 12, pp. 4323–4332, 2006.

[10] F. M. Ghannouchi, O. Hammi, and M. Helaoui, *Behavioral Modeling and Predistortion of Wideband Wireless Transmitters*. John Wiley & Sons, Inc., Hoboken, NJ, 2015.

[11] A. Saleh, "Frequency-independent and frequency-dependent nonlinear models of twt amplifiers," *IEEE Transactions on Communications*, vol. 29, no. 11, pp. 1715–1720, 1981.

[12] A. Ghorbani and M. Sheikhan, "The effect of solid state power amplifiers (sspas) nonlinearities on mpsk and m-qam signal transmission," in *1991 Sixth International Conference on Digital Processing of Signals in Communications*, 1991, pp. 193–197.

[13] C. Rapp, "Effects of hpa-nonlinearity on a 4-dpsk/ofdm-signal for a digital sound broadcasting system." 1991.

[14] "RAQ issue 195: A guide for choosing the right RF amplifier for your application," https://www.analog.com/en/analog-dialogue/raqs/raq-issue-195.html, accessed: 2022-02-25.

[15] E. Raei, M. Alaee-Kerahroodi, and B. S. M. R., "Beampattern shaping for coexistence of cognitive MIMO radar and MIMO communications," in *2020 IEEE 11th SAM*, 2020, pp. 1–5.

[16] M. Hong, M. Razaviyayn, Z.-Q. Luo, and J.-S. Pang, "A unified algorithmic framework for block-structured optimization involving big data: With applications in machine learning and signal processing," *IEEE Signal Processing Magazine*, vol. 33, no. 1, pp. 57–77, 2016.

[17] A. Aubry, A. De Maio, A. Zappone, M. Razaviyayn, and Z.-Q. Luo, "A new sequential optimization procedure and its applications to resource allocation for wireless systems," *IEEE Transactions on Signal Processing*, vol. 66, no. 24, pp. 6518–6533, 2018.

[18] J. Nutini, M. Schmidt, I. Laradji, M. Friedlander, and H. Koepke, "Coordinate descent converges faster with the gauss-southwell rule than random selection," in *International Conference on Machine Learning*, 2015, pp. 1632–1641.

[19] (2022) Digital predistorter. [Online]. Available: https://nl.mathworks.com/help/comm/ref/comm.dpd-system-object.html

[20] K.-J. Kim. (2022, Nov.) Modeling RF power amplifiers and increasing transmitter linearity with DPD using MATLAB. modelling-rf-power-amplifiers-with-dpd-using-matlab-white-paper.pdf. [Online]. Available: https://www.mathworks.com/content/dam/mathworks/white-paper/